THE EFFECT OF La CONCENTRATION ON THE STRUCTURAL AND ELECTRONIC PROPERTIES OF TETRAGONAL PZT USING FIRST PRINCIPLES CALCULATION

Nur Amirah Aniesya Azemi¹, Mohamad Fariz Mohamad Taib^{2,3}, Nur Hafiz Hussin^{1,3*}

¹Faculty of Applied Sciences
Universiti Teknologi MARA UiTM Pahang, 26400 Bandar Tun Abdul Razak Jengka, Pahang
Malaysia

²Faculty of Applied Sciences
Universiti Teknologi MARA, 40450 Shah Alam, Selangor, Malaysia

*Corresponding author: hafizhussin@uitm.edu.my

Abstract

The effect of Lanthanum (La) concentration on the structural and electronic properties of tetragonal Lead Zirconate Titanate, PbZrTiO₃ (PZT) were investigated in this study using first-principles calculation. Since lead (Pb) is recognised as a toxic substance with serious consequences for human health and the environment, La-doped PZT was selected to be examined. Lead-free elements have been considered potential substitute materials for ferroelectric components in PZT (PbZrTiO₃). This study aims to investigate and understand the structural and electronic properties of pure PZT. La was chosen as a dopant to study its effect on the electronic and structural PZT properties. First-principle calculations based on density functional theory (DFT) incorporated into the CASTEP software were used to accomplish the computations. Different exchange-correlation functional approximations, such as the Local Density Approximation (LDA-CAPZ) and the Generalised Gradient Approximation (GGA-PBE and GGA-PBEsol), were used to determine the geometry optimisation of ferroelectric phase materials. The lattice parameter and structure volume values calculated by GGA-PBE for PZT were the most precise. Additionally, the outcomes of tetragonal PZT were comparable to those of experiments. Hence, GGA-PBE was selected for La-doped PZT based on comparing the tetragonal PZT's lattice parameter with experiment data and selecting GGA-PBE as the most accurate. The best composition of La was 40%, with a lower band gap of 0.641 eV. By substituting or doping in a Pb-based system, these results will help experimentalists reduce the amount of lead they use, significantly advancing the field of green technology.

Keywords: density functional theory, electronic properties, first principle calculation, PZT

Introduction

The production of improved materials has been crucial to technological growth. The technology was made compact, portable and high-performing based on the primary needs of numerous users in technical applications, including ultra-sensitive actuators, sensors, ultrasonic transducers and piezoelectrics. Material scientists and engineers were inspired by these requirements to develop new materials that could enhance the capabilities of already-existing technology. Various material properties control these current technologies, ferroelectricity being one of them. The unique dielectric properties of Rochelle salt were first discovered around 100 years ago, giving rise to the current idea of basic ferroelectricity. Many Published by University Teknologi Mara (UiTM) Cawangan Pahang – September 2023 | 45

useful features, including high dielectric permittivity, pyroelectric, piezoelectric and bulk photovoltaic capabilities, have been discovered in ferroelectric materials, which also have a highly sensitive polar structure and spontaneous polarisation below Curie temperature (T_c) that is electrically switchable (Yao et al., 2022). Materials with a perovskite-based structure are ideal for ferroelectric and piezoelectric use as ferroelectric research advances continuously. As far as commercial piezoelectric materials go, the members of the Lead Zirconium Titanate (PZT) class have been the most successful and are still the most widely used owing to their beneficial properties and reasonable costs (Guo et al., 2020). Lead zirconate titanate (PZT) is a typical perovskite "ABO₃" piezoelectric material. PZT exhibits noticeably high piezoelectric characteristics in this morphotropic phase boundary (MPB) area (Hong et al., 2022). Ferroelectric lanthanum-doped lead zirconate titanate (PLZT) of perovskite type is an intriguing material close to the morphotropic phase boundary (MPB) owing to its significant remnant polarisation and electro-optic effects. It displays a significantly greater electro-optical impact than LiNbO₃, which is frequently used in industrial waveguide devices (Baedi et al., 2010). The PZT ceramic's densification rates are accelerated by adding lanthanum, creating poreless, homogeneous microstructures. Hysteresis loops with an extremely high coercive field are visible in PLZT ceramic compositions in the tetragonal ferroelectric zone. Materials with this composition behave linearly in electro-optics for an electric field lower than the critical electric field (E<E_C).

In this study, the structural properties of pure PZT in a tetragonal structure, including lattice parameters and volume, as well as the impact of La doping on these properties, were reported and analysed. First-principles calculations were carried out to understand the properties of pure PZT and the effect of the La impurity in PZT. A density functional theory was employed using the Cambridge Serial Total Energy Package (CASTEP) to comprehend the lanthanum doping influence on the other properties of lead zirconate titanate. Since lead is a toxic ferroelectric material that is harmful to the environment and human body, Pb-based material PZT was modified by substituting doping at the A-site with La, which is numerically anticipated to enhance the ferroelectric properties as well as eventually reduce the consumption of Pb in the electroactive device.

Computational Method

In this research, the structural and electronic properties of tetragonal pure PZT and the effect of different concentrations of La to PZT were investigated using a fully implemented computational method by the software Material Studio 2020 (MS 2020). The MS Visualiser was used in structure building for pure PZT, 0.2 La-doped PZT, 0.4 La-doped PZT, 0.6 La-doped PZT and 0.8 La-doped PZT, while the structural and electronic properties are calculated using MS Cambridge Serial Total Energy Package (CASTEP) code which is based on the density functional theory (DFT). Convergence tests were first carried out first with the convergence of energy change per atom <5×10–6 eV, residual force <0.01 eV/Å, stress <0.02 GPa and displacement of atoms <0.0005 Å (Alam et al., 2020). The k-point used for each compound of PZT and PLaZT for tetragonal structures was 4x4x4 with 350 eV cut-off energy Monkhorst Pack (Yaakob et al., 2012).

Results and Discussion

Structural Properties of Tetragonal PZT and PLZT

The crystal structures of tetragonal pure PZT undoped La and La-doped PZT with different concentrations of La are shown in **Figure 1**. PZT and PLZT crystal structures were formed in a 1x1x2 supercell. For the structure of La-doped PZT, the Pb atom changed its concentration with the addition of different concentrations of La. The value of the lattice parameter and volume of the tetragonal structure of pure PZT and La-doped PZT was optimised from the estimated geometry optimisation to study the effect of La concentration in PZT through several functionals, including GGA-PBE, GGA-PBEsol and LDA-CAPZ as listed in **Table 1**. Therefore, the lattice parameters of a (Å), b (Å) and c (Å) of pure PZT were compared with experimental data, as reported by Noheda et al. (2008).

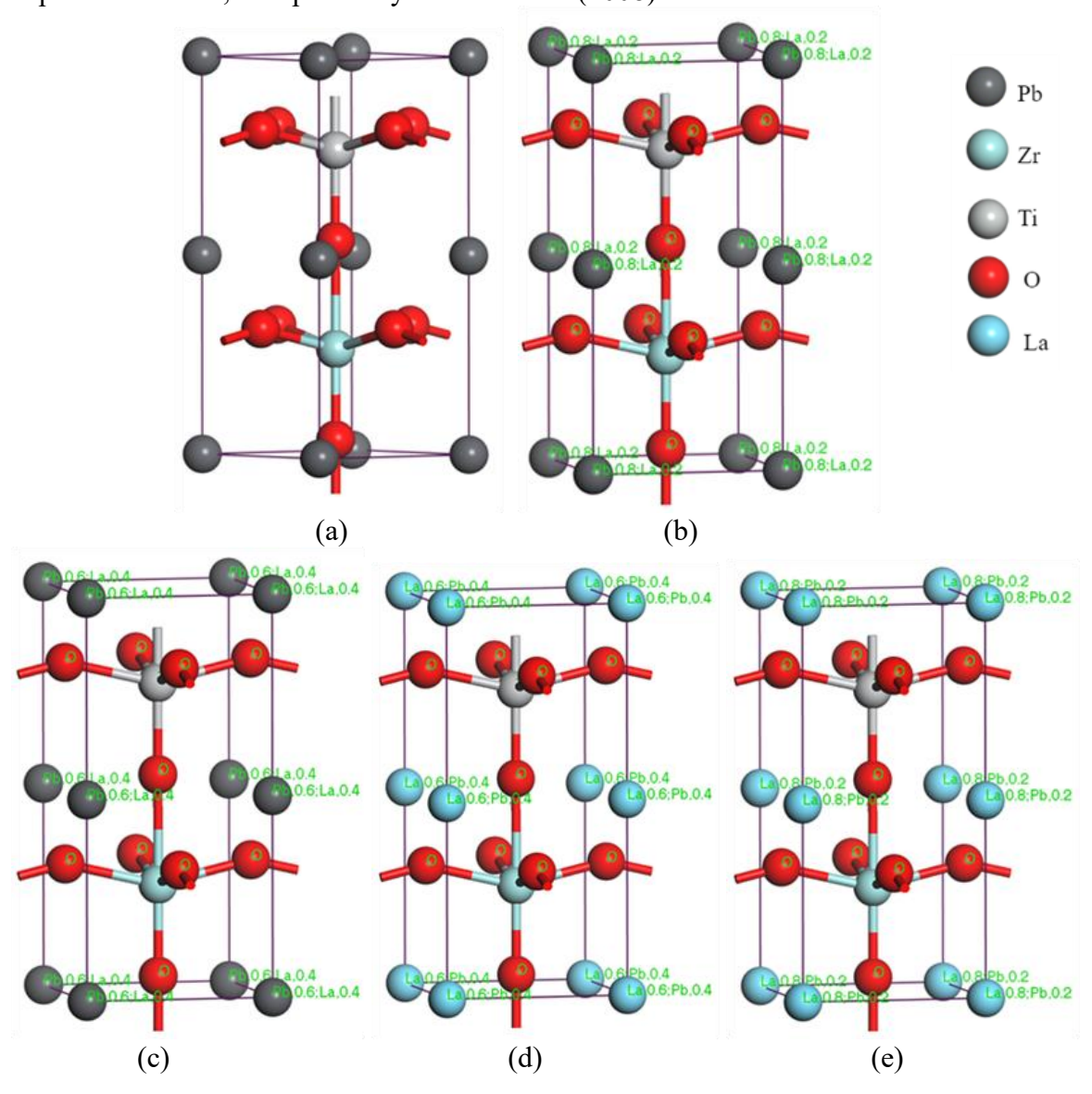


Figure 1 The crystal structure of tetragonal (a) PbZrTiO₃ (b) Pb_{0.8}La_{0.2}ZrTiO₃ (c) Pb_{0.6}La_{0.4}ZrTiO₃ (d) Pb_{0.4}La_{0.6}ZrTiO₃ (e) Pb_{0.2}La_{0.8}ZrTiO₃

Table 1 Lattice Parameter and Volume for Tetragonal pure PZT and La-doped PZT with different concentrations of La.

PbZrTiO ₃	GGA-PBE	GGA-PBEsol	LDA-CAPZ	*Exp (Noheda
				et. al., 2008)
<i>a</i> (Å)	4.011	4.004	3.971	4.046
	(-0.865%)	(-1.038%)	(-1.854%)	
b (Å)	4.011	4.004	3.971	4.046
	(-0.865%)	(-1.038%)	(-1.854%)	
c (Å)	8.875	8.407	8.271	4.139
	(114.424%)	(103.117%)	(99.831%)	
$V(A^3)$	142.801	134.807	130.444	-
Pb _{0.8} La _{0.2} ZrTiO ₃				
a (Å)	4.085	4.029	3.982	-
b(A)	4.085	4.029	3.982	-
c (Å)	8.236	8.131	8.065	-
$V(A^3)$	137.423	132.020	127.902	-
Pb _{0.6} La _{0.4} ZrTiO ₃				
a (Å)	4.573	4.393	4.349	-
b(A)	4.573	4.393	4.349	-
c (Å)	7.456	7.638	7.632	-
$V(A^3)$	151.918	143.395	139.970	-
Pb _{0.4} La _{0.6} ZrTiO ₃				
a (Å)	4.168	4.110	4.061	-
b (Å)	4.168	4.110	4.061	-
c (Å)	7.985	7.928	7.886	-
$V(A^3)$	138.730	133.914	130.055	-
Pb _{0.2} La _{0.8} ZrTiO ₃				
a (Å)	4.084	4.020	3.972	-
b (Å)	4.084	4.020	3.972	-
c(A)	8.251	8.213	8.179	-
$V(A^3)$	137.636	132.742	129.042	

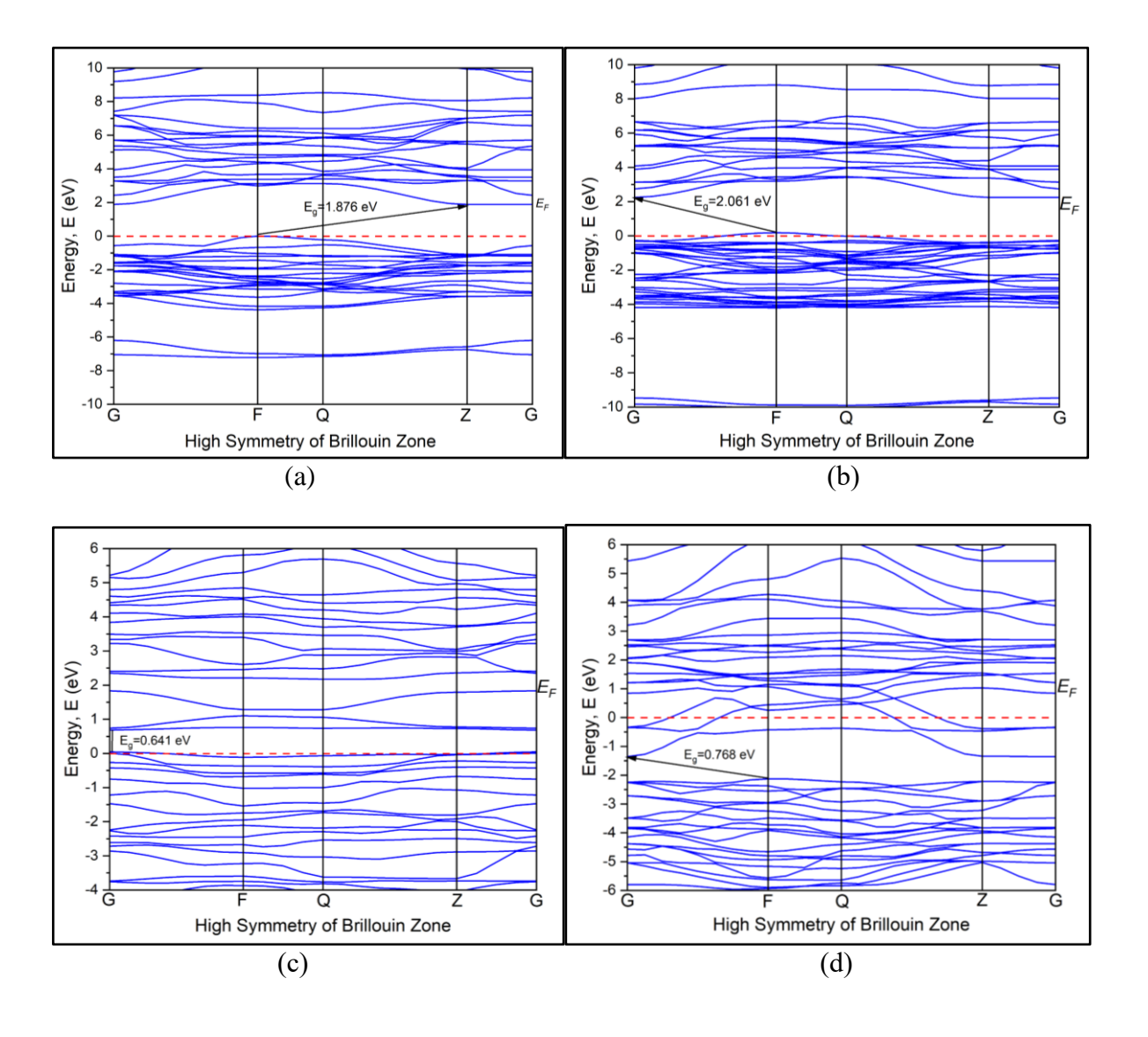
From the calculated lattice parameter listed in Table 1, only GGA-PBE can potentially optimise the La-doped PZT since three functionals have optimised the pure PZT, while the GGA-PBE has a lattice parameter value similar to the experimental. The optimised lattice parameters for pure PZT using GGA-PBE were a=b=4.011 Å and c=8.875 Å, slightly different from the experimental one with a=b=4.046 Å, c=4.139 Å and was about -0.865% for lattice a. The difference between the lattice a for GGA-PBEsol was around -1.038%, and the LDA-CAPZ difference was approximately -1.854%. With a difference of less than 1%, this finding shows that the functional GGA-PBE may best be compatible with experimental results. There was also no difference between La-doped and undoped PZT due to the ionic size of La, which is comparable to the ionic size of Pb. The results show that La is the best candidate to reduce the usage of Pb in the PZT.

Energy Band Structure of Tetragonal PZT and PLZT

The calculated electronic band structures for tetragonal pure PZT and La-doped PZT using the GGA-PBE functional are illustrated for the energy ranges of 30 to 20 eV, respectively, along

the direction of the high symmetry Brillouin zone (G–F–Q–Z–G) in Figure 2-6. The red dashed line represents the Fermi level. As earlier mentioned, the O 2p states that have been hybridised with Pb were primarily responsible for the highest valence band (VB) located at the Fermi level (E_F) at 0 eV for PZT and La-doped PZT. Meanwhile, Ti 3d atoms represent the majority of the lowest conduction band (CB) for these materials.

According to the electronic band gap calculation, the indirect band gap for tetragonal pure PZT was 1.876 eV at the F-Z point, according to **Figure 2**. However, the indirect electronic band gaps at the F-G point for 0.2 La, 0.6 La, and 0.8 La are 2.061 eV, 0.768 eV, and 1.828 eV, respectively, as shown in Figures 3, 5 and 6. On the other hand, 0.4 La has a direct band gap of about 0.641 eV at the G point (**Figure 4**). The findings indicate that adding La-doped PZT reduced the band gap value. Therefore, it may be concluded that doping La into pure PZT changed the band structure, especially at CB and VB. 0.4 La-doped with PZT has a smaller band gap than other dopants, which is good for ferroelectric properties.



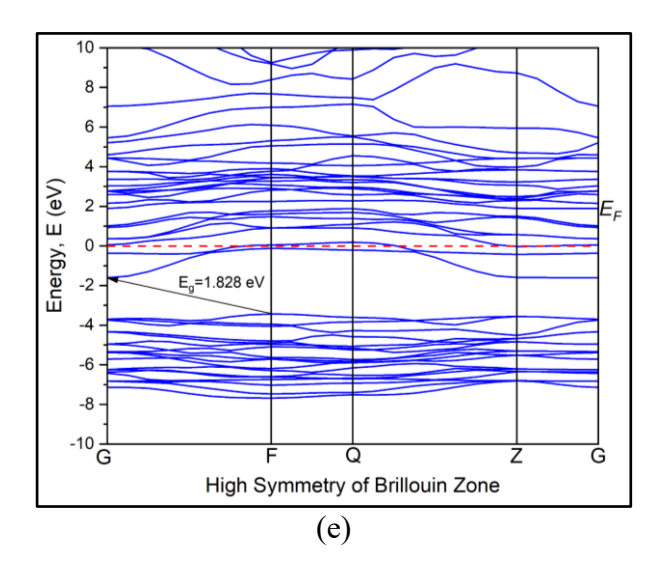


Figure 2 Energy Band Structure of (a) PbZrTiO₃ (b) Pb_{0.8}La_{0.2}ZrTiO₃ (c) Pb_{0.6}La_{0.4}ZrTiO₃ (d) Pb_{0.4}La_{0.6}ZrTiO₃ (e) Pb_{0.2}La_{0.8}ZrTiO₃

Density of states (DOS) of Tetragonal PZT and PLZT

After optimising the structure, the total and partial DOS of pure PZT and La-doped PZT were also calculated to better understand the chemical bonds between those materials. The distribution of elements in each orbital was analysed using the partial and total density of states (DOS), as well as the most significant peaks in the DOS, whether they are from s, p, or d characters, were identified. Figure 7-11 illustrates that the predicted total DOS's energy range was between (EF -60 eV) and (EF +40 eV). It is clear that the valence band and conduction band of pure PZT are made up of O 2p states and Ti 3d states. The Fermi level is indicated by the dashed line at zero energy. As a result, the valence band extended from 0 eV to the left while the conduction band extended from 0 eV to the right. The GGA-PBE functional, the most dependable functional, was employed in the computation, just like the band structure. According to Figure 7, the electron O 2p orbital dominated the highest valence band of tetragonal pure PZT, while Ti 3d and Zr 4d states were mostly attributable to the lowest conduction band. For 0.2 La-doped PZT, the Ti 3d and Pb 6p La 5p orbitals dominated the conduction band, whereas the electron O 2p orbital dominated the valence band (Figure 8). O 2p orbital was the highest valence band in 0.4 La-doped PZT, as shown in Figure 9, and Pb La 5d likewise existed in this band. However, electrons will excite from O 2p to the lowest conduction band, which consists of Pb La 5d, Ti 3d and Zr 4d. Pb La 5d, Ti 3d and Zr 4d were the three main elements in the conduction band. When PZT was doped with 0.6 La, as shown in Figure 10, the conduction band moved below the Fermi level, with Pb La 5d dominating, then Ti 3d and Zr 4d. The O 2p orbital dominated the valence band. Furthermore, the O 2p valence bond dominated 0.8 La-doped PZT, whereas the highest Pb La 6s orbital was found in the conduction band, followed by Ti 3d and Zr 4d (Figure 11).

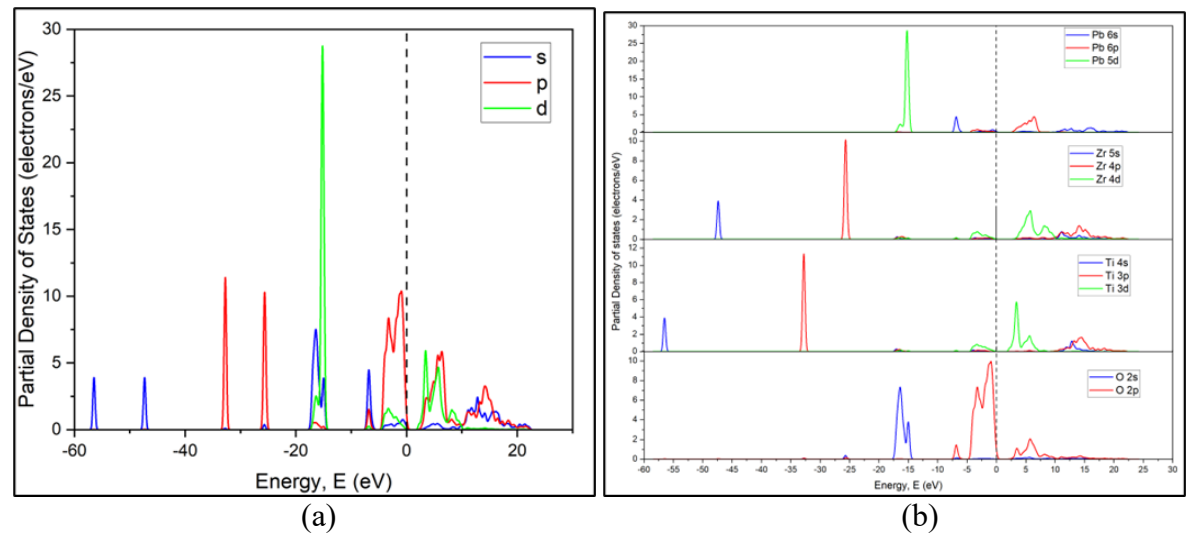


Figure 7 Partial Density of States (PDOS) of (a) PbZrTiO₃ (b) Pb, Zr, Ti and O atoms

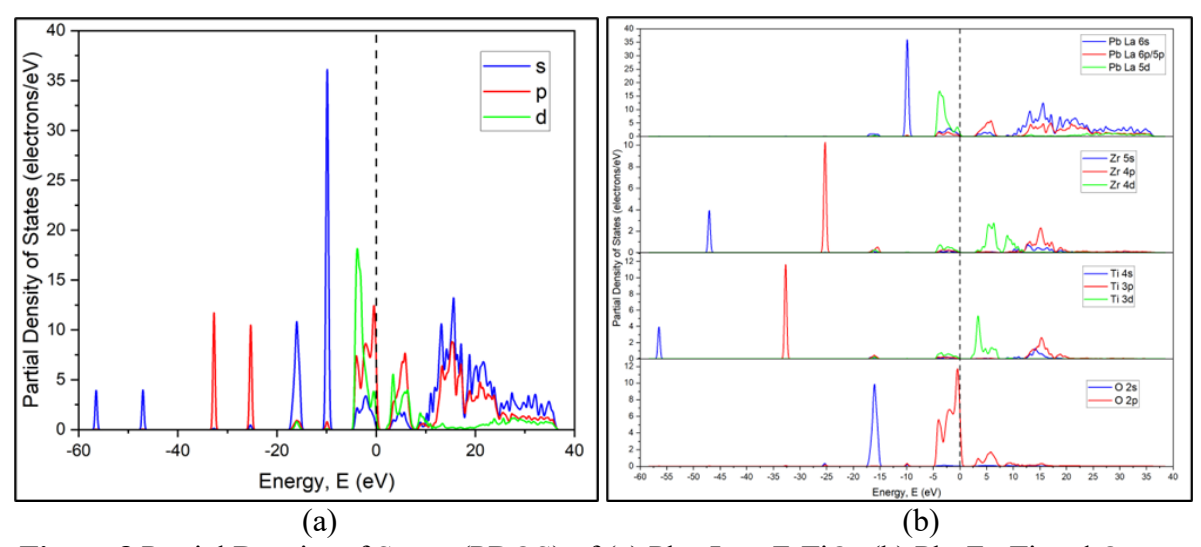


Figure 8 Partial Density of States (PDOS) of (a) Pb_{0.8}La_{0.2}ZrTiO₃ (b) Pb, Zr, Ti and O atoms

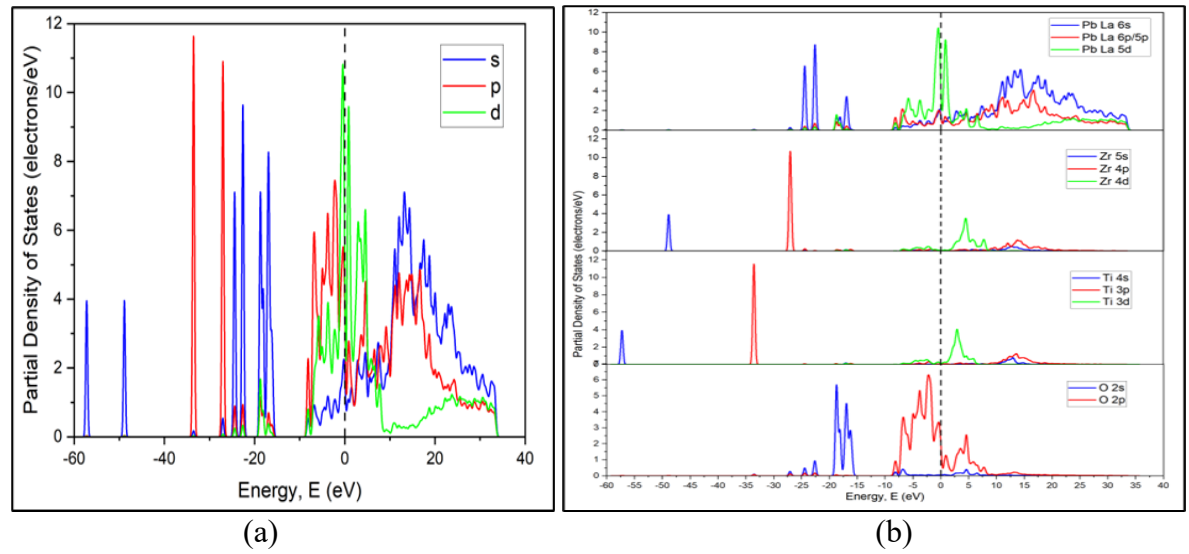


Figure 9 Partial Density of States (PDOS) of (a) Pb_{0.6}La_{0.4}ZrTiO₃ (b) Pb, Zr, Ti and O atoms

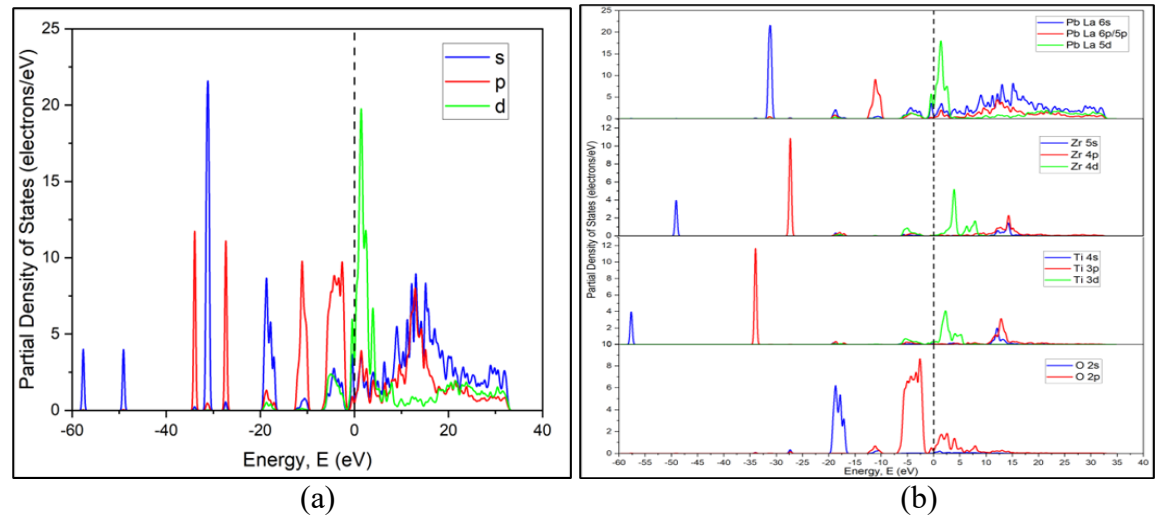


Figure 10 Partial Density of States (PDOS) of (a) Pb_{0.4}La_{0.6}ZrTiO₃ (b) Pb, Zr, Ti and O atoms

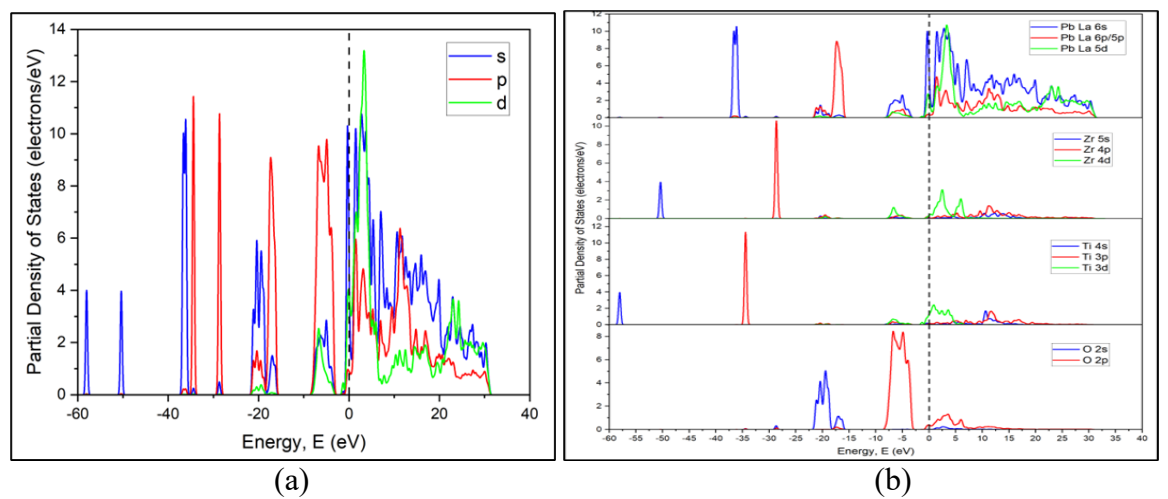


Figure 11 Partial Density of States (PDOS) of (a) Pb_{0.2}La_{0.8}ZrTiO₃ (b) Pb, Zr, Ti and O atoms

Conclusion

In conclusion, the best functionality for the tetragonal structure was GGA-PBE for pure PZT and PLZT with different concentrations of La, respectively. Using DFT, the energy band structure was also derived. The 0.4 La-doped PZT has the lowest band gap, measuring 0.641 eV. The conduction band will, however, narrow to the valence band due to the dopant of La. The PDOS and sum of DOS for the density of states were calculated using DFT. It was discovered that the valence band, namely O 2p-dominated in all pure and doped PZT, was dominant there for concentrations of 0.2 La, Ti 3d and Zr 4d. The valence band, dominated by Pb La 5d, Ti 3d and Zr 4d for PZTs with 0.4 and 0.6 La-doped, shifted narrowly from the conduction band for these PZTs. In the conduction band, Ti 3d and Zr 4d were dominant in 0.8 La-doped PZT with Pb La 6s. Therefore, it can be inferred that the substance is a semiconductor, while the ideal dopant concentration for lanthanum doping into PZT is 0.4 La-doped PZT.

Authors Contribution

Castep Software Trainer - Dr Mohamad Fariz Mohamad Taib; Supervision - Dr Nur Hafiz Hussin

Acknowledgement

Above all, I would like to thank my supervisor, Dr. Nur Hafiz Hussin for his support and guide me to complete my research.

Conflict of interests

The author declares that there is no conflict of interests.

References

- Baedi, J., Benam, M. R., & Majidiyan, M. (2010). First-principles study of the effect of La substitution on the electronic and optical properties of. *Physica Scripta*, 81(3). https://doi.org/10.1088/0031-8949/81/03/035701
- Batra, V., Kotru, S., Varagas, M., & Ramana, C. V. (2015). Optical constants and band gap determination of Pb_{0.95}La_{0.05}Zr_{0.54}Ti_{0.46}O₃ thin films using spectroscopic ellipsometry and UV-visible spectroscopy. *Optical Materials*, 49(October), 123–128. https://doi.org/10.1016/j.optmat.2015.08.019
- Behara, S., Poonawala, T., & Thomas, T. (2021). Crystal structure classification in ABO₃ perovskites via machine learning. In *Computational Materials Science* (Vol. 188). https://doi.org/10.1016/j.commatsci.2020.110191
- Bochenek, D., Niemiec, P., & Dercz, G. (2020). The effect of mixed doping on the microstructure and electrophysical parameters of the multicomponent PZT-type ceramics. *Materials*, *13*(8). https://doi.org/10.3390/MA13081996
- Chen, Y., Li, L., Zhou, Z., Wang, Y., Chen, Q., & Wang, Q. (2023). La₂O₃ modified BiYbO₃ Pb(Zr,Ti)O₃ ternary piezoelectric ceramics with enhanced electrical properties and thermal depolarization temperature. *Journal of Advanced Ceramics*, 1–39. https://doi.org/10.26599/jac.2023.9220774
- Gözüaçık, N. K., Mensur-Alkoy, E., & Alkoy, S. (2019). Effects of lanthanum doping on electrical and electromechanical properties of (Pb_{1-x}La_x)(Zr_{0.70}Ti_{0.30})O₃ ceramics. *Journal of Materials Science: Materials in Electronics*, 30(15), 14045–14052. https://doi.org/10.1007/s10854-019-01769-0
- Guo, J., Zhou, H., Fan, T., Zhao, B., Shang, X., Zhou, T., & He, Y. (2020). Improving electrical properties and toughening of PZT-based piezoelectric ceramics for high-power applications via doping rare-earth oxides. Journal of Materials Research and Technology, 9(6), 14254–14266. https://doi.org/10.1016/j.jmrt.2020.10.022

- Hasan, M., Nasrin, S., Islam, M. N., & Hossain, A. K. M. A. (2022). First-principles insights into the electronic, optical, mechanical, and thermodynamic properties of lead-free cubic ABO₃[A = Ba, Ca, Sr; B = Ce, Ti, Zr] perovskites. *AIP Advances*, *12*(8). https://doi.org/10.1063/5.0104191
- Hong, I. G., Kim, J. H., Shin, H. Y., Chung, C. Y., Paik, U. G., & Im, J. in. (2022). Dependence of local atomic structure on piezoelectric properties of PbZr_{1-x}Ti_xO₃ materials. *Journal of Asian Ceramic Societies*, 10(2), 514–519. https://doi.org/10.1080/21870764.2022.2079807
- Hussin, N. H., Taib, M. F. M., Samat, M. H., Jon, N., Hassan, O. H., & Yahya, M. Z. A. (2017). Study of Structural, Electronic and Optical Properties of Lanthanum Doped Perovskite PZT Using Density Functional Theory. *Applied Mechanics and Materials*, 864, 127–132. https://doi.org/10.4028/www.scientific.net/amm.864.127
- Jing, Y., & Aluru, N. R. (2020). The role of A-site ion on proton diffusion in perovskite oxides (ABO₃). In *Journal of Power Sources* (Vol. 445). https://doi.org/10.1016/j.jpowsour.2019.227327
- Kumar, A., Kim, S. H., Peddigari, M., Jeong, D. H., Hwang, G. T., & Ryu, J. (2019). High Energy Storage Properties and Electrical Field Stability of Energy Efficiency of (Pb_{0.89}La_{0.11})(Zr_{0.70}Ti_{0.30})_{0.9725}O₃ Relaxor Ferroelectric Ceramics. *Electronic Materials Letters*, 15(3), 323–330. https://doi.org/10.1007/s13391-019-00124-z
- Kumari, N., Monga, S., Arif, M., Sharma, N., Sanger, A., Singh, A., Vilarinho, P. M., Gupta, V., Sreenivas, K., Katiyar, R. S., & Scott, J. F. (2019). Multifunctional behavior of acceptor-cation substitution at higher doping concentration in PZT ceramics. In Ceramics International (Vol. 45, Issue 10). https://doi.org/10.1016/j.ceramint.2019.03.138
- Md Jahangir Alam, N. N., Ab Malik Marwan, N. A., Samat, M. H., Mohyedin, M. Z., Hussin, N. H., Marwan Ali, A. M., Hassan, O. H., Yahya, M. Z. A., & Mohamad Taib, M. F. (2020). First Principles Study on Structural and Electronic Properties of Cubic (Pm3m) And Tetragonal (P4mm) ATiO3 (A=Pb, Sn). *Scientific Research Journal*, 17(2), 149. https://doi.org/10.24191/srj.v17i2.9918
- Sahu, N., & Panigrahi, S. (2011). Mathematical aspects of Rietveld refinement and crystal structure studies on PbTiO3 ceramics. *Bulletin of Materials Science*, *34*(7), 1495–1500. https://doi.org/10.1007/s12034-011-0349-0
- Sanchez, A., Zambrano, C., Procel, L. M., & Stashans, A. (2003). *Structural and Electronic Properties of PZT. August*, 310–316. https://doi.org/10.1117/12.515782
- Schileo, G., & Grancini, G. (2021). Lead or no lead? Availability, toxicity, sustainability and environmental impact of lead-free perovskite solar cells. *Journal of Materials Chemistry C*, 9(1), 67–76. https://doi.org/10.1039/d0tc04552g
 - Published by University Teknologi Mara (UiTM) Cawangan Pahang September 2023 | 54

- Sharma, R. K. (2021). Dielectric Properties of Modified Lead Zirconate Titanate. 16(2), 237–243.
- Siddiqui, M., Mohamed, J. J., & Ahmad, Z. A. (2020). Structural, piezoelectric, and dielectric properties of PZT-based ceramics without excess lead oxide. *Journal of the Australian Ceramic Society*, *56*(2), 371–377. https://doi.org/10.1007/s41779-019-00337-3
- Sturge, M. D. (2020). Electrons and Holes in Semiconductors. *Statistical and Thermal Physics*, 269–290. https://doi.org/10.1201/9781315275529-19
- Toriyama, M. Y., Ganose, A. M., Dylla, M., Anand, S., Park, J., Brod, M. K., Munro, J. M., Persson, K. A., Jain, A., & Snyder, G. J. (2022). How to analyse a density of states. *Materials Today Electronics*, *1*, 100002. https://doi.org/10.1016/J.MTELEC.2022.100002
- Yao, K., Chen, S., Lai, S. C., & Yousry, Y. M. (2022). Enabling Distributed Intelligence with Ferroelectric Multifunctionalities. *Advanced Science*, *9*(1), 1–30. https://doi.org/10.1002/advs.202103842
- Yaakob, M. K., Taib, M. F. M., & Yahya, M. Z. A. (2012). First Principle Study of Dynamical Properties of a New Perovskite Material Based on GeTiO₃. Advanced Materials Research, 501, 352–356.